Fault-Tolerant Operation of an Open-End Winding Five-Phase PMSM Drive with Short-Circuit Inverter Fault

Ngac Ky Nguyen, Fabien Meinguet, Eric Semail, *Member, IEEE* and Xavier Kestelyn

***Abstract*—Multi-phase machines are well-known for their fault tolerant capability. Star-connected multiphase machines have fault tolerance in open-circuit. For inverter switch short-circuit fault, it is possible to keep a smooth torque of Permanent Magnet Synchronous Machine (PMSM) if the currents of faulty phases are determined and their values are acceptable. This paper investigates fault-tolerant operations of an open-end f ve-phase drive, i.e. a multi-phase machine fed with a dual-inverter supply. Inverter switch short-circuit fault is considered and handled with a simple solution. Original theoretical developments are presented. Simulation and experimental results validate the proposed strategy.**

***Index Terms*—AC drives, Control reconfiguration Fault-tolerance, Multi-phase machines, Open-end winding, PMSM, Reliability.**

I. Introduction

RELIABITILY OF DRIVES is a key parameter in some critical applications and its improvements can be obtained in various ways. With a conservative design, one solution is to use the system below its maximum functioning point, and therefore its expected lifetime increases thanks to oversizing. However, in this case, system efficien y may be reduced and the cost of the system usually increases, especially when the range of power is significant Moreover, if a fault finall happens, the system cannot continue to work even at reduced power. This is particularly true since power electronics component failures are yet mostly unpredictable [1].

To increase the drive availability, fault-tolerance has been introduced in the last decades. Fault-tolerance can be applied to the inverter [2]–[9] and/or to the electric machine [10]–[13]. Specifi configuration of three-phase and multi-phase drives have been investigated for their properties in healthy and faulty conditions.

Multi-phase drives have additional degrees of freedom compared with traditional three-phase drives [14]. These degrees of freedom can be used for different purposes, such as additional torque generation or fault tolerance when a part of the system fails. Fault detection and control reconfiguratio of the drive in case of open-circuit faults have been extensively studied in the past years [15]–[29]. On the other hand, only a few works have addressed the problem of inverter switch short-circuit faults [6], [30], except in topologies with additional components such as fuses and parallel thyristors which are not used in healthy operations [2]–[5].

In [6], the authors investigate a three-phase drive topology with an open-end winding machine and a dual-inverter supply. The authors show that fault tolerance against open-circuit fault requires a zero-sequence path for the current (connection between inverters). On the other hand, inverter switch short-circuit faults can be handled by creating an artificia neutral point through the faulty inverter. In the latter case, this reconfiguratio cannot be applied if there is a zero-sequence path. Therefore, a complete fault tolerance cannot be achieved without additional devices which connect or disconnect both inverters depending on the condition of the drive.

These issues can be solved with an open-end f ve-phase drive supplied by two independent voltage sources since the machine can be operated with open-circuit faults without zero-sequence path. This topology, illustrated in Fig.1, has already been investigated in [31] where the authors propose a space vector modulation technique.

The present paper deals with the fault-tolerant capability of an open-end winding f ve-phase PMSM drive following a short-circuit inverter fault. Various degrees of reconfiguratio are investigated, starting from no reconfiguratio up to a full reconfiguratio (control algorithm and gate signals).

It is assumed that the inverter is equipped with smart drivers that are able to locate a short-circuit fault almost instantaneously and to remove the gate signal of the complementary switch to avoid a short-circuit of the DC source [32], [33].

In section II, the drive modeling is presented, highlighting the zero-sequence component which is of paramount importance for control reconfiguration Section III develops a simple modulation strategy and the control algorithms for the healthy and faulty conditions. Inverter switch short-circuit faults are addressed in detail. Simulation results are reported in section IV. Finally, the test bed is presented in section V and experimental results validate the theoretical part.

II. Drive modeling

The topology under study is shown in Fig. 1, which consists of two isolated voltage sources, two f ve-leg inverters and a

Manuscript received June 11, 2014; revised September 8, 2014 and October 16, 2014; accepted November 18, 2014.

N. K. Nguyen, E. Semail and X. Kestelyn are with the Laboratory of Electrical Engineering and Power Electronics of Lille (L2EP), Arts et Métiers ParisTech, Lille Cedex, France, e-mail: [ngacky.nguyen, xavier.kestelyn, eric.semail]@ensam.eu.

F. Meinguet is with the Thales Alenia Space - Thales Group, Belgium, email: fabien.meinguet@thalesaleniaspace.com.

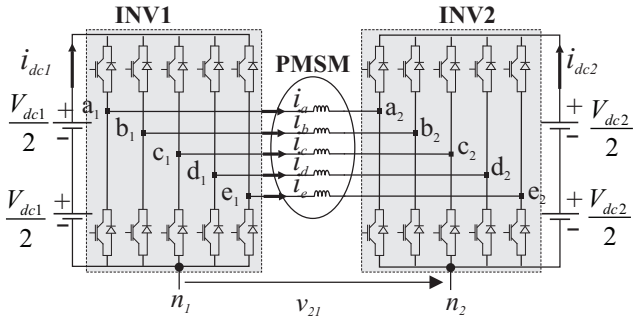

Fig. 1. Drive topology

f ve-phase open-end winding PMSM. We consider $V_{dc1} = V_{dc2} = \frac{1}{2}V_{dc}$ in this study but a general case where V_{dc1} is different to V_{dc2} can be possible.

Let us define

$$[\mathbf{v}] = \begin{bmatrix} v_a & v_b & v_c & v_d & v_e \end{bmatrix}^T \quad (1)$$

$$[\mathbf{i}] = \begin{bmatrix} i_a & i_b & i_c & i_d & i_e \end{bmatrix}^T \quad (2)$$

$$[\mathbf{e}] = \begin{bmatrix} e_a & e_b & e_c & e_d & e_e \end{bmatrix}^T \quad (3)$$

where $[\mathbf{v}]$ is the voltage vector, $[\mathbf{i}]$ is the current vector and $[\mathbf{e}]$ is the back-electromotive force (back-EMF) vector of the PMSM machine.

Assuming no magnetic saturation and no saliency, the voltage equations are given by:

$$[\mathbf{v}] = R_s[\mathbf{i}] + [\mathbf{L}]\frac{d[\mathbf{i}]}{dt} + [\mathbf{e}] \quad (4)$$

where:

$$[\mathbf{L}] = \begin{bmatrix} L & M_1 & M_2 & M_2 & M_1 \\ M_1 & L & M_1 & M_2 & M_2 \\ M_2 & M_1 & L & M_1 & M_2 \\ M_2 & M_2 & M_1 & L & M_1 \\ M_1 & M_2 & M_2 & M_1 & L \end{bmatrix} \quad (5)$$

with R_s as the stator resistance, L, M_1 and M_2 as the stator self and mutual inductances. The references of electric potential are n_1 and n_2 for the inverter 1 and the inverter 2, respectively (see Fig. 1). Hence:

$$[\mathbf{v}] = [\mathbf{v}_{INV1}] - [\mathbf{v}_{INV2}] - [\mathbf{v}_{21}] \quad (6)$$

where $[\mathbf{v}_{21}] = \begin{bmatrix} v_{21} & v_{21} & v_{21} & v_{21} & v_{21} \end{bmatrix}^T$ and v_{21} is the voltage between n_1 and n_2 (see Fig. 1). $[\mathbf{v}_{INV1}]$ and $[\mathbf{v}_{INV2}]$ are the voltage vectors of the two inverters and they are define as:

$$[\mathbf{v}_{INV1}] = \begin{bmatrix} v_{a_1n_1} & v_{b_1n_1} & v_{c_1n_1} & v_{d_1n_1} & v_{e_1n_1} \end{bmatrix}^T \quad (7)$$

$$[\mathbf{v}_{INV2}] = \begin{bmatrix} v_{a_2n_2} & v_{b_2n_2} & v_{c_2n_2} & v_{d_2n_2} & v_{e_2n_2} \end{bmatrix}^T \quad (8)$$

As there is no path for the zero-sequence current, the sum of all phase currents is equal to zero:

$$[\mathbf{n}]^T[\mathbf{i}] = \mathbf{0} \quad (9)$$

where $[\mathbf{n}] = \begin{bmatrix} 1 & 1 & 1 & 1 & 1 \end{bmatrix}^T$.

Applying Concordia and Park transformations to equation (4), the modeling of the system expressed in the stator and rotor reference frames is obtained, with notations $\alpha_1\beta_1\alpha_2\beta_20$ and $d_1q_1d_2q_20$ respectively. For the topology under study, the inverter has 2^{10} different combinations of states. The corresponding vectors are depicted in Fig. 2 (a) and (b) for the subspaces associated with the fundamental $\alpha_1\beta_1$ and third-harmonic $\alpha_2\beta_2$ components respectively. More details about the subspace vector theory are given in [34].

The zero-sequence voltage component is calculated as follows:

$$v_0 = \frac{1}{\sqrt{5}}[\mathbf{n}]^T[\mathbf{v}] \quad (10)$$

Substituting (4) and (9) into (10) yields:

$$v_0 = e_0 \quad (11)$$

where e_0 is the zero-sequence of the back-EMF and can be calculated in the same way as (10).

An analytical expression of v_{21} is obtained by substituting (6) into (4) and calculating the zero-sequence component:

$$v_{21} = \frac{1}{\sqrt{5}}v_{0,eq} - \frac{1}{\sqrt{5}}e_0 \quad (12)$$

with $v_{0,eq}$ the zero-sequence voltage of an equivalent inverter which would have a connection between the two negative potentials (n_1 and n_2) of the DC-buses. That is:

$$v_{0,eq} = \frac{1}{\sqrt{5}}([\mathbf{n}]^T([\mathbf{v}_{INV1}] - [\mathbf{v}_{INV2}])) \quad (13)$$

(13) shows that $v_{0,eq}$ depends on the instantaneous output voltage of the inverters. As the result, $v_{0,eq}$ is a control variable, whereas v_0 (or e_0) is not.

It is worth noticing that (12) is similar to the expression obtained for a star connection [12]. In the latter case, the neutral-point floatin voltage is affected by the zero-sequence of the back-EMF and the inverter output voltage, while for the topology under study it is v_{21}.

As v_{21} is associated with the zero-sequence component, it has no effect on the $\alpha\beta$ components and the space vector theory can be applied by omitting v_{21} in the calculation of these components.

The electromagnetic torque of the PMSM is given by:

$$T_{em} = \frac{1}{\Omega}[\mathbf{e}]^T[\mathbf{i}] \quad (14)$$

with Ω as the mechanical speed.

III. Control strategy

This section describes the control strategy used for the experimental tests. First, the modulation strategy is briefl described. This modulation strategy is common to all control schemes (healthy and faulty). No modificatio of this strategy is required for the post-fault operation.

Next, the control strategy in healthy operation is briefl addressed, followed by the control strategies with an inverter-switch short-circuit fault.

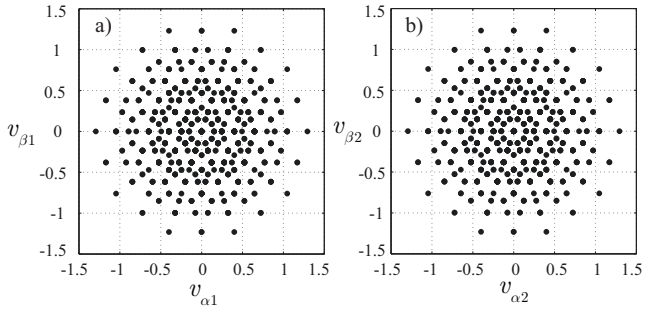

Fig. 2. Voltage vectors in the stator reference frame (normalized by $V_{dc} = 2V_{dc1} = 2V_{dc2}$). Left: Subspace associated with the fundamental component (a). Right: Subspace associated with the third-harmonic component (b).

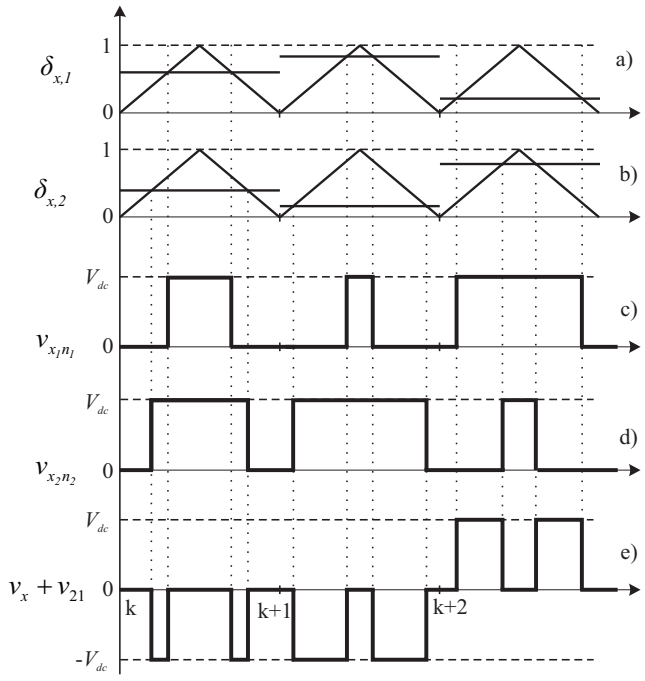

Fig. 3. Carrier-based modulation strategy: a) Switching function of the x_1-leg; b) Switching function of the x_2-leg; c) Voltage of the x_1 leg $v_{x_1 n_1}$; d) Voltage of the x_2 leg $v_{x_2 n_2}$; e) Sum voltage $v_x + v_{21}$.

A. Modulation strategy

A space-vector modulation of an open-end winding five phase machine is reported in [31]. In this paper, a very simple modulation strategy is chosen for this application, i.e. a centered PWM strategy with the duty cycles $\delta_{x,1}$ and $\delta_{x,2}$ calculated as follows ($x \in (a, b, c, d, e)$):

$$\delta_{x,1} = \frac{1}{2}\left(\frac{v_x^*}{V_{dc}} + 1\right) \tag{15}$$

$$\delta_{x,2} = \frac{1}{2}\left(-\frac{v_x^*}{V_{dc}} + 1\right) = 1 - \delta_{x,1} \tag{16}$$

with v_x^* the x-phase voltage reference ($-V_{dc} \leq v_x^* \leq V_{dc}$).

An example is given in Fig. 3, showing the modulation functions, the triangular carrier and the resulting voltage of $v_x + v_{21}$ (in healthy condition, $v_{21} = 0$). Usually, this technique of modulation allows to double the apparent carrier frequency of PWM (see Fig. 3 e)) and the current ripples are thus reduced.

B. Control strategy in healthy operation

Fig. 4 shows the general scheme for torque control. The Park current references are obtained by equation (17). It can be noticed that this choice is to obtain simplified current control loops. The PMSM is fed by voltage resulting from a strategy which is based on faulty information. If all phases are healthy, then v_{21} is set to 0. As the results, the voltage references are identical with the ones obtained by current regulators. This corresponds to the 'healthy' position of the switch in Fig. 4.

In the Park reference frame, the currents can be obtained by:

$$[\mathbf{i}]_{\text{Park}} = \sqrt{\frac{2}{5}}\,[\mathbf{R}]^T\,[\mathbf{C}]^T\,[\mathbf{i}] \tag{17}$$

with:

$$[\mathbf{C}] = \begin{bmatrix} \frac{1}{\sqrt{2}} & 1 & 0 & 1 & 0 \\ \frac{1}{\sqrt{2}} & \cos\frac{2\pi}{5} & \sin\frac{2\pi}{5} & \cos\frac{4\pi}{5} & \sin\frac{4\pi}{5} \\ \frac{1}{\sqrt{2}} & \cos\frac{4\pi}{5} & \sin\frac{4\pi}{5} & \cos\frac{8\pi}{5} & \sin\frac{8\pi}{5} \\ \frac{1}{\sqrt{2}} & \cos\frac{6\pi}{5} & \sin\frac{6\pi}{5} & \cos\frac{12\pi}{5} & \sin\frac{12\pi}{5} \\ \frac{1}{\sqrt{2}} & \cos\frac{8\pi}{5} & \sin\frac{8\pi}{5} & \cos\frac{16\pi}{5} & \sin\frac{16\pi}{5} \end{bmatrix} \tag{18}$$

$$[\mathbf{R}] = \begin{bmatrix} 1 & 0 & 0 & 0 & 0 \\ 0 & \cos\theta_e & -\sin\theta_e & 0 & 0 \\ 0 & \sin\theta_e & \cos\theta_e & 0 & 0 \\ 0 & 0 & 0 & \cos 3\theta_e & \sin 3\theta_e \\ 0 & 0 & 0 & -\sin 3\theta_e & \cos 3\theta_e \end{bmatrix} \tag{19}$$

This transformation leads to two d-q rotating frames [35]. The first frame is associated with the first harmonic and rotates at $\omega = \frac{d\theta_e}{dt}$, and the second one is associated with the third harmonic and rotates at -3ω. To keep the control scheme simple, the calculation of the current references is obtained from the torque reference and the fundamental component of the back-EMF. This simplification leads to:

$$[\mathbf{i}]^*_{\text{Park}} = \begin{bmatrix} I_0^* = 0 \\ I_{d1}^* = 0 \\ I_{q1}^* = \frac{T_{em}^*}{e_{q1}} \\ I_{d2}^* = 0 \\ I_{q2}^* = 0 \end{bmatrix} \tag{20}$$

Proportional-Integral (PI) controllers are used for the current control, along with an EMF feed-forward compensation.

The zero-sequence voltage can be chosen in order to increase the DC-link voltage utilization by injecting voltage harmonic components which are multiples of five. However, the choice in this paper is to maintain the value of $v_{21} = 0$ in a healthy operation. Therefore, from (12), the zero-sequence voltage of the equivalent inverter is given by:

$$v_{0,eq,H} = e_0 \tag{21}$$

where H is a subscript which refers to the healthy operation. (21) is possible since the zero-sequence current cannot circulate. As a consequence, even if a fifth harmonic of EMF exists it is not necessary to compensate the zero-sequence current. If only one DC voltage source is used for the two inverters, the

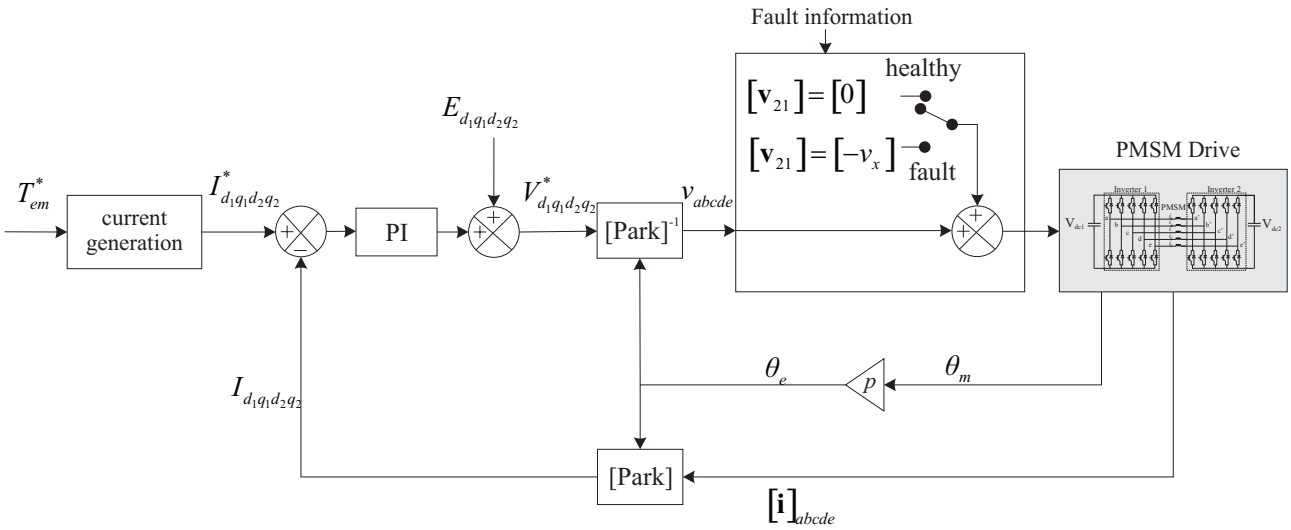

Fig. 4. Control block diagram in a healthy condition and in a faulty condition where $x = a, b, c, d, e$ corresponding to faulty phase.

zero-sequence current could exist and a supplementary control is thus required.

C. Control strategy with one short-circuit fault (inverter switch)

It is possible to deal with a shorted switch fault with the topology under study. Under switch fault condition, it is assumed that the complementary switch is maintained 'open' in order to avoid a short-circuit of the associated DC source.

Hence the number of switch combinations decreases to $2^9 = 512$. It is however difficul to develop a post-fault strategy considering a specifi subset of vectors and a simple modulation strategy. Therefore, four reconfiguratio techniques are investigated in the following sections.

1) Without reconfigu ation: it might be interesting to test the fault-tolerant capability of the drive without any change of the control algorithms and modulation strategies.

The main problem in this case is that the converter output voltage is different from the controller reference voltage. As one leg is connected permanently to the positive or negative bus, a voltage DC component appears at the faulty-phase terminals. The controller will try to reject this component (which is rotating at the electrical frequency in the rotor reference frames) and therefore the response depends on the controller and machine parameters. However, injecting a voltage DC component yields a current that is only limited by the stator resistance. Hence, large currents are expected.

2) Wye-coupling realization of a faulty inverter: in order to mitigate the effects of the fault, a simple solution is to realize a star connection by setting all the top (if one top switch is faulty) or bottom (if one bottom switch is faulty) IGBTs of the faulty inverter to 1 [6]. In this case, a classical structure is obtained where the PMSM is fed by only one f ve-phase inverter. The limit of voltage of a star connection is reported in Fig. 6. The modulation technique can be either classical PWM or SVM. With the PWM, the maximum voltage is equal to $0.5V_{dc}$ while it can reach $\frac{4}{5}\cos\frac{pi}{5}V_{dc}$ [31] with the SVM.

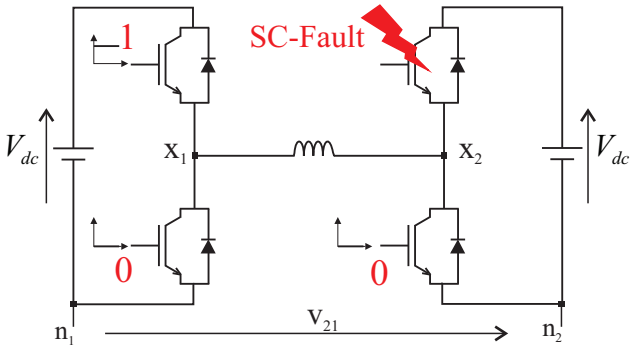

Fig. 5. Reconfiguratio of the inverter legs in case of inverter short-circuit fault (top switch of the x_2-leg where x can be a, b, c, d or e).

In this paper, this solution is not presented because it has been already studied.

3) Simple reconfigu ation: Fig. 5 gives an example where the top switch of the leg x_2 is short-circuited ($v_{x_2n_2} = V_{dc}$). A simple reconfiguratio can be achieved by connecting the top switch of the leg x_1 to the positive bus. If the bottom switch of the leg x_2 is faulty, then the bottom switch of the leg x_1 should be connected to the negative bus. Indeed, in case of short-circuit fault, x_1 and x_2 are required to have the same potential. This configuratio can be obtained by hardware implementation (error signal and additional logic drive the gate signals of the other leg) or control signal (duty cycle equals '1' or '0'). The machine voltage vector in this case is shown in Fig. 6. In order to maintain the same operating point as without any fault, the voltage magnitude has to be preliminarily kept within the limit of the voltage of the faulty case. If the machine is operated at rated power before the fault, it is clear that there is an unavailable area since the short-circuit occurs and the speed (or torque) has to be reduced to put the voltage vector below the new limits. In our study, all tests will be carried out below the limit of voltage in short-circuit fault. The idea is to show how can we configur the controllers to maintain a constant torque in case of fault.

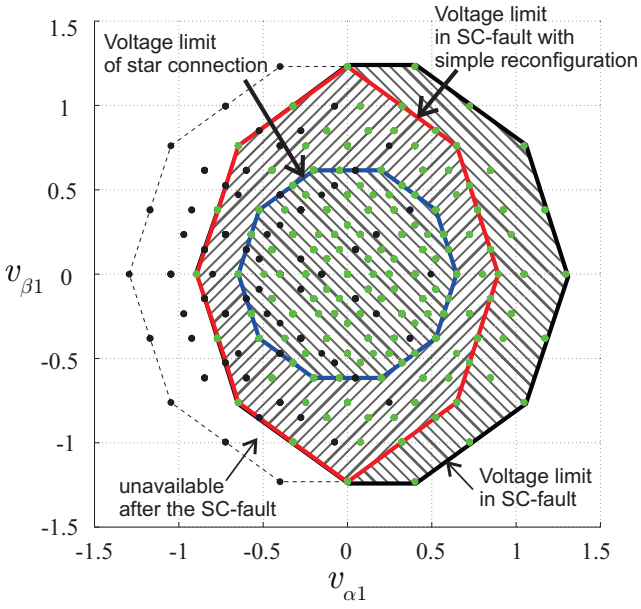

Fig. 6. Limits of machine voltage in $\alpha_1\beta_1$ plan (normalized by V_{dc}) in case of SC-fault (top switch of the a_1 -leg) with and without a simple reconfiguration

The advantage of this strategy is that the average value of v_x (x: faulty phase) is equal to zero so there is no DC component to be rejected by the controller. On the other hand, there is still a difference between the reference voltage and the inverter output voltage. As a consequence, the drive response is again dependent on the controller and machine parameters.

4) Simple reconfigu ation with control scheme improvement (full reconfigu ation): to mitigate the aforementioned problem, the controller has to impose a voltage reference which can be generated by the inverter. To do so, the reconfiguratio of Fig. 5 applies as well. However, an additional change in the control scheme is mandatory. The 'fault' position of the switch is chosen (see Fig. 4) for a full reconfiguration Mathematical developments will be given below to justify this choice.

Considering Fig. 5 and (6) and assuming that the faulty phase is the phase-a, an important and simple result is:

$$v_a = -v_{21} \tag{22}$$

(22) shows that the faulty-phase voltage is equal to the difference of potentials between n_1 and n_2. From (12) this voltage can be controlled with the zero-sequence voltage of the equivalent inverter.

The Concordia transformation has the following expression:

$$\begin{bmatrix} v_a \\ v_b \\ v_c \\ v_d \\ v_e \end{bmatrix} = \sqrt{\frac{2}{5}}[\mathbf{C}] \begin{bmatrix} v_0 \\ v_{\alpha 1} \\ v_{\beta 1} \\ v_{\alpha 2} \\ v_{\beta 2} \end{bmatrix} \tag{23}$$

and substituting (12) and (22) into (23) yields:

$$v_{0,eq,SC_a} = -\sqrt{2}v_{\alpha 1} - \sqrt{2}v_{\alpha 2} \tag{24}$$

As the objective is to maintain a constant torque, i.e. no modificatio of the $d_1q_1d_2q_2$ currents (or equivalently the $\alpha_1\beta_1\alpha_2\beta_2$ currents), the $d_1q_1d_2q_2$ voltages (or equivalently the $\alpha_1\beta_1\alpha_2\beta_2$ voltages) have to be maintained as well. Eq. (24) shows that a modificatio of the zero-sequence voltage allows this condition to be obtained.

From (23) and (24), the phase-a voltage reference is expressed as the following (after the fault):

$$v^*_{a-\mathrm{F}} = \frac{1}{\sqrt{5}}v_{0,eq,SC_a} + \sqrt{\frac{2}{5}}(v_{\alpha 1} + v_{\alpha 2}) = 0 \tag{25}$$

The phase-b voltage reference is then calculated as follows (where F stands for 'Faulty' and H stands for 'Healthy'):

$$v^*_{b-\mathrm{F}} = \frac{1}{\sqrt{5}}v_{0,eq,SC_a} + v^*_{b-\mathrm{H}} \tag{26}$$

(12) and (22) lead to:

$$v^*_{b-\mathrm{F}} = -v^*_{a-\mathrm{H}} + v^*_{b-\mathrm{H}} = u^*_{ba-\mathrm{H}} \tag{27}$$

In the same way, voltage references of the other phases are:

$$v^*_{c-\mathrm{F}} = -v^*_{a-\mathrm{H}} + v^*_{c-\mathrm{H}} = u^*_{ca-\mathrm{H}} \tag{28}$$

$$v^*_{d-\mathrm{F}} = -v^*_{a-\mathrm{H}} + v^*_{d-\mathrm{H}} = u^*_{da-\mathrm{H}} \tag{29}$$

$$v^*_{e-\mathrm{F}} = -v^*_{a-\mathrm{H}} + v^*_{e-\mathrm{H}} = u^*_{ea-\mathrm{H}} \tag{30}$$

It's interesting to show that the voltage references of the PMSM machine under short-circuit fault (inverter switch) can be easily obtained to maintain the same operating point as before the fault. In this case, the line-line voltages are used instead of the phase voltages. The Tab. I gives different voltage reference vectors corresponding to each phase short-circuit fault. A summary of the reconfiguratio modes for the cases under study is given in Tab. II.

D. Analyses of voltage limits and torque-speed characteristic

In the above sections, two solutions have been presented for an inverter switch SC-fault. In order to highlight the feasibility of these proposed solutions, an analysis of the limits in term of voltage and torque-speed characteristic available after the fault should be pointed out.

As summarized in Tab. I, the proposed strategy needs to supply a motor phase with a line-line voltage in faulty mode instead of a line-neutral voltage in healthy mode in order to maintain the rated torque in steady-state degraded mode. Then,

TABLE I
VOLTAGES REFERENCE OF MACHINE UNDER SHORT-CIRCUIT FAULT OF DIFFERENT PHASES

Short-circuit	Voltage reference vector under fault condition
Phase a	$[\mathbf{v}]^*_{\mathrm{F}} = \begin{bmatrix} 0 & u^*_{ba-H} & u^*_{ca-H} & u^*_{da-H} & u^*_{ea-H} \end{bmatrix}$
Phase b	$[\mathbf{v}]^*_{\mathrm{F}} = \begin{bmatrix} u^*_{ab-H} & 0 & u^*_{cb-H} & u^*_{db-H} & u^*_{eb-H} \end{bmatrix}$
Phase c	$[\mathbf{v}]^*_{\mathrm{F}} = \begin{bmatrix} u^*_{ac-H} & u^*_{bc-H} & 0 & u^*_{dc-H} & u^*_{ec-H} \end{bmatrix}$
Phase d	$[\mathbf{v}]^*_{\mathrm{F}} = \begin{bmatrix} u^*_{ad-H} & u^*_{bd-H} & u^*_{cd-H} & 0 & u^*_{ed-H} \end{bmatrix}$
Phase e	$[\mathbf{v}]^*_{\mathrm{F}} = \begin{bmatrix} u^*_{ae-H} & u^*_{be-H} & u^*_{ce-H} & u^*_{de-H} & 0 \end{bmatrix}$

TABLE II
SUMMARY OF THE CONTROL PARAMETERS FOR THE VARIOUS RECONFIGURATION MODES UNDER STUDY (A-PHASE FAULT)

Mode of operation	$v_{x,1} = v_{x,2}$	$v^*_{0,eq}$
Healthy (H_0)	no	e_0
Short-circuit and no reconfigu ration	no	e_0
Short-circuit and simple recon- f guration	yes	e_0
Short-circuit and full reconfig uration	yes	$-\sqrt{2}(v_{\alpha 1} + v_{\alpha 2})$

the new peak phase voltage is increased by $\sqrt{3}$ in faulty mode which means that the voltage source inverter (VSI) has to be able to deliver these new voltage references. To do this, some precautions have to be made at the beginning of the drive's design. First, the choice of the DC bus's voltage has to be available in faulty mode. Secondly, the PMSM has to be designed to be fed by a new voltage ($\sqrt{3}$ times greater) in faulty mode. This is not a real constraint thanks to an adapted insulation material.

As the new voltage references increase, the apparent power (kVA) per phase has to be oversized concerning the voltage capability. In fact, the oversizing is already necessary without considering fault-mode operation when the system must be able to work in transient operation with a large increase of the current in inductive circuit. Inductive voltage drop must be then supplied by increasing the duty cycle of the VSI. As consequence, the calculation of the necessary rated voltage is not obvious, inducing thus safety margin calculation that can be used to give the ability to work in fault mode but of course with reduced ability for transient operations. From this point of view, a drive's design for the faulty mode can be achieved without an additional oversizing since the inverter has already been oversized at the beginning.

It can be noticed that since the torque and speed are maintained as in healthy mode, the active powers of the machine and the battery do not change, i.e there is no an oversizing of the battery and the PMSM. For simulation and experimentation presented in this work, the DC bus is adapted for functioning in both modes (healthy and faulty). In the healthy operation, the magnitude of the duty cycle is small. In the faulty mode, this magnitude is increased until the required line-line voltages (per healthy phases) are obtained.

IV. SIMULATION RESULTS

For simulation, the speed-normalized back-EMF of the machine is given in Fig. 7. The other parameters are reported in Tab. III. The rotor speed is set to 1500 rpm and the torque is equal to half of the rated torque. A short-circuit inverter fault is generated by setting the upper IGBT control signal of the phase-a equal to 1 at $t = 0.02$ s.

Simulation results are reported in Fig. 8 and Fig. 9. Before the fault, the machine torque tracks the reference and the

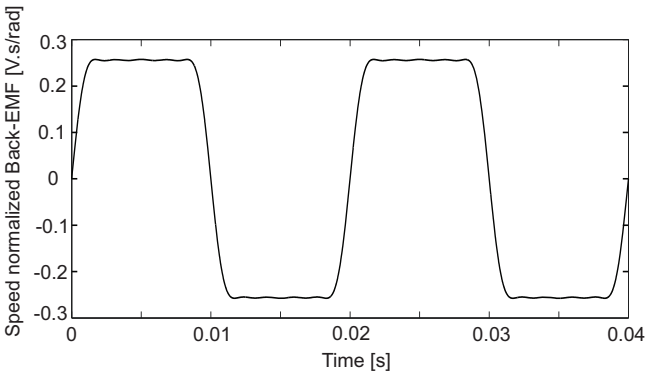

Fig. 7. Speed-normalized back-EMF of machine for simulation.

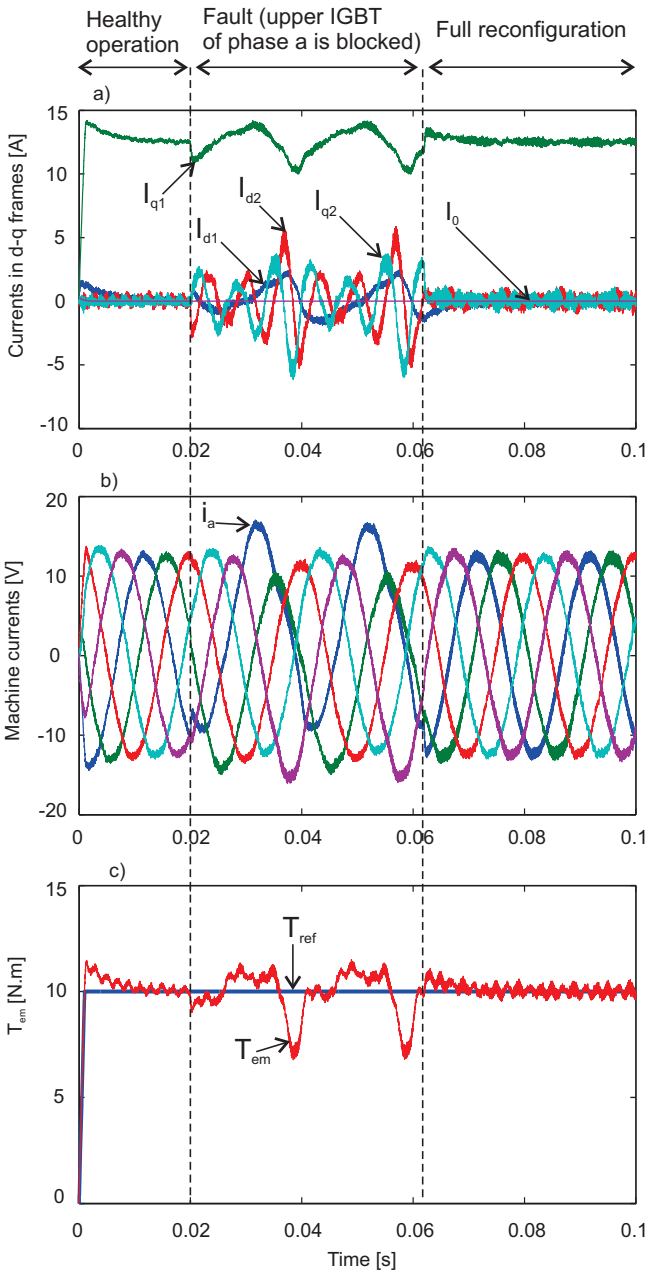

Fig. 8. Simulation results of full reconfiguration a) Machine currents in rotor reference frame; b) Machine currents [A]; c) Torque [N.m].

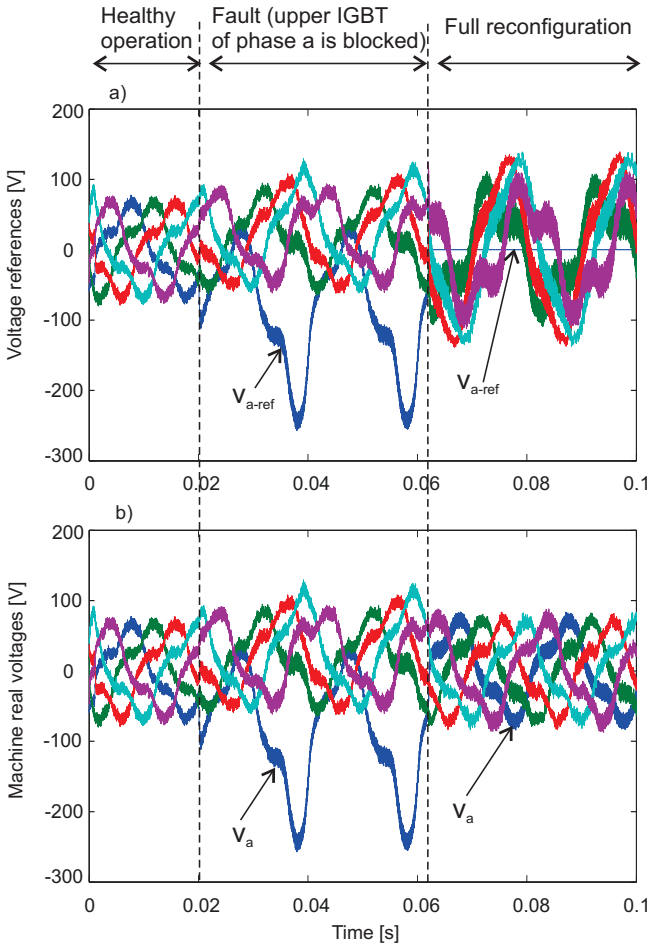

Fig. 9. Simulation results of full reconfiguration a) Voltage references [V]; b) Machine real voltages [V].

currents are sinusoidal because the current reference I_{q2}^{*} is set to zero. The machine voltages contain the 3rd harmonic to compensate the same rank of the back-EMF induced by the magnet. The voltage references are equal to the real machine voltages.

A short-circuit of the upper IGBT of the phase-a is activated at $t = 0.02$ s. During 0.04 s, from $t = 0.02$ s to $t = 0.06$ s, there is no action for correcting this fault. The currents expressed in the rotor frame (I_{d1}, I_{q1}, I_{d2} and I_{q2}) start oscillating and create torque pulsations. The phase-a current presents a DC component that leads to a very high peak of voltage of this phase. It is obvious that this high value of peak can deteriorate the machine coils and power electronic components of the inverters. At $t = 0.06$ s, a full reconfigu ration is enabled. The torque ripple is canceled, the currents in stator frame become balanced again and the result of their transformation in rotor frame is constant. By observing the voltage references and the real voltages of the machine in Fig. 9, after a full correction, the voltage reference for the faulty phase (the phase-a) is set to zero. For four healthy phases, the references are line-line voltages and the real voltages behave as in the healthy operation. These simulation results justify the theory developed in section III-C4. It can be noted that the DC-bus voltage is large enough to feed a line-line voltage in fault condition. In practice, if the machine is operated at rated point before the fault, it is obvious that the speed and/or torque has to be reduced to keep the voltage below the new limit (see Fig. 6). The next section gives experimental results.

V. Experimental Results

A. Test-bed description

A picture of the test-bed is shown in Fig. 10. The system consists of a five-phase double-ended PMSM, two five-leg inverters and two isolated DC-sources. A dSPACE1005 board is used for control prototyping. The load is an electromagnetic powder brake.

The switch short-circuit fault is emulated by forcing the corresponding duty cycle to '1' or '0'. The machine parameters are given in Tab. III. The back-EMF waveform is almost trapezoidal, as shown in Fig. 11.

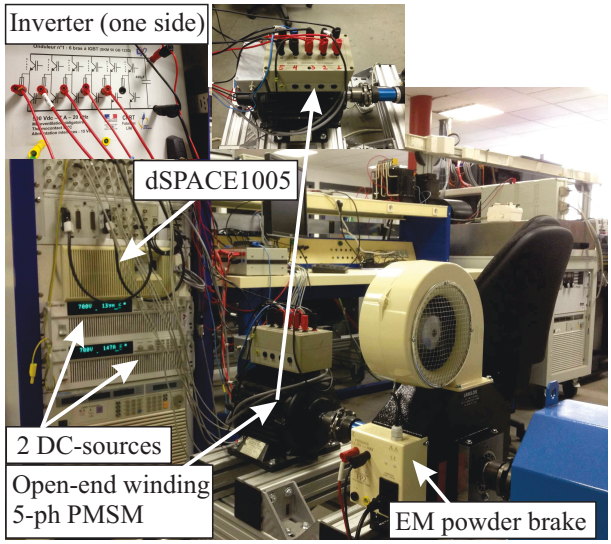

Fig. 10. Experimental platform.

TABLE III
Machine Parameters under Experimental Tests

Parameters	Values
R_s	2.24 Ω
$L_{d1} = L_{q1}$	3.2 mH
$L_{d3} = L_{q3}$	0.9 mH
e_{q1}/Ω	0.51 V.s.rad^{-1}
Pole pairs number (p)	2
Nominal speed	1500 rpm
Nominal current	15 A
Nominal torque	20 N.m
Nominal power	3.1 kW

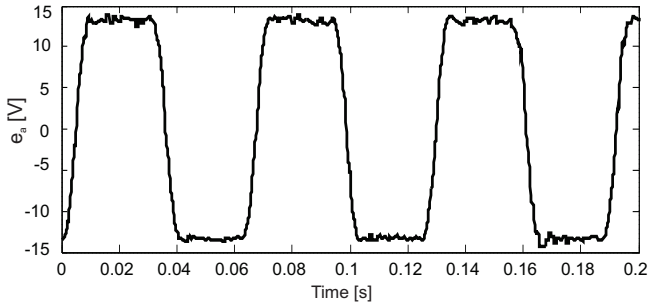

Fig. 11. Back-EMF of the five-phase machine at $\Omega = 50$ rad/s.

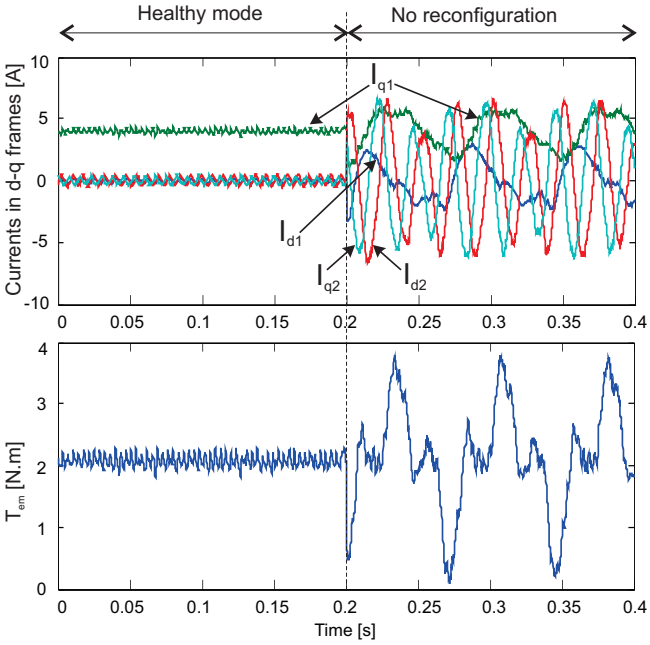

Fig. 12. Inverter switch short-circuit fault and no reconfig ration (experimental results). Top: currents expressed in the rotor reference frame. Bottom: Electromagnetic torque (calculated from the model).

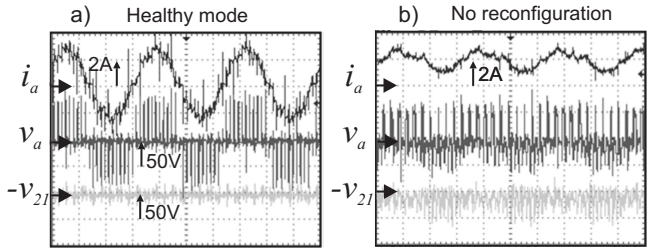

Fig. 13. Healthy operation (a) and no reconfiguratio after the fault (b). Scope results showing the a-phase current i_a, the a-phase voltage v_a and the voltage between the two inverter DC-bus v_{21}.

B. Control with an inverter short-circuit fault

1) No reconfigu ation: Fig. 12 and Fig. 13 show experimental results of the control with an inverter switch short-circuit fault and no reconfiguratio at rotor speed $\Omega = 42$ rad/s. The fault occurs at time $t = 0.2$ s. Fig. 12 shows that the current magnitudes in the d_2q_2 subspace increase a lot following the occurrence of the fault. A torque ripple of about 165% appears due to the fault. Fig. 13 a) shows

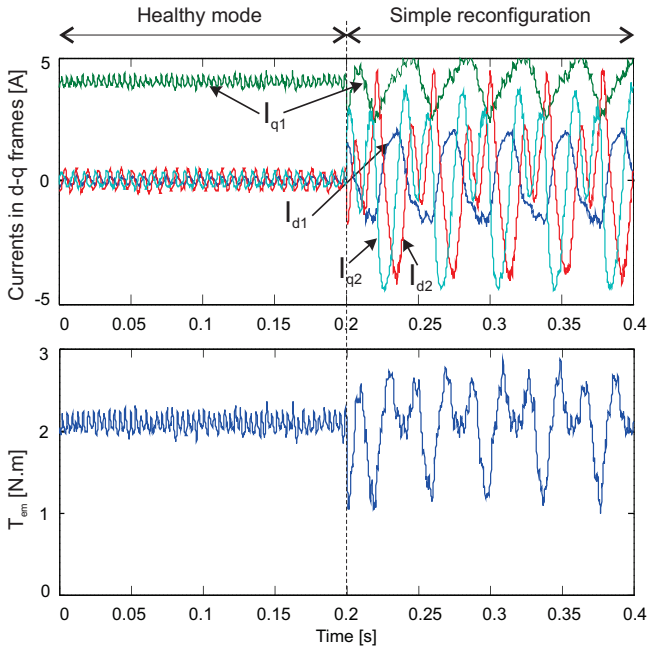

Fig. 14. Inverter switch short-circuit fault and simple reconfiguratio (experimental results). Top: currents expressed in the rotor reference frame. Bottom: Electromagnetic torque (calculated from the model).

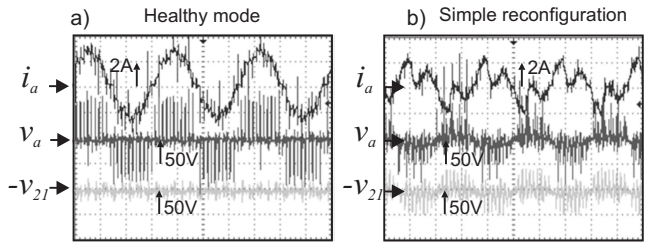

Fig. 15. Healthy operation (a) and simple configuratio (b). Scope results showing the faulty a-phase current i_a, the a-phase voltage v_a and the voltage between the two inverter DC-bus v_{21}.

the scope results in the healthy operation. The phase current i_a is sinusoidal, lagging the phase voltage v_a. The voltage difference between the two inverter DC-links v_{21} is also measured. It can be seen that v_{21} is close to zero (average and instantaneous values), as expected from the control algorithm in proper mode. Fig. 13 b) shows the scope results upon short-circuit inverter fault. The faulty phase current i_a has a positive DC component, while v_a and v_{21} are seriously affected by the fault.

2) Simple reconfigu ation: Fig. 14 and Fig. 15 show experimental results of the control with an inverter switch short-circuit fault and simple reconfiguratio ($\Omega = 40$ rad/s). The fault occurs at time $t = 0.2$ s. A torque ripple of about 75% appears due to the fault. The scope results of Fig. 15 show that the faulty phase current is quite distorded, but its magnitude is rather low. It can be noticed that this fault induces the supply of the secondary machine associated with the subspace $\alpha_2\beta_2$ (I_{d2} and I_{q2} are different to zero). So in order to obtain a constant torque, new current references (voltages) of the two fictitiou machines in Concordia reference frame have to be determined. When a fault occurs in the inverter, a simple

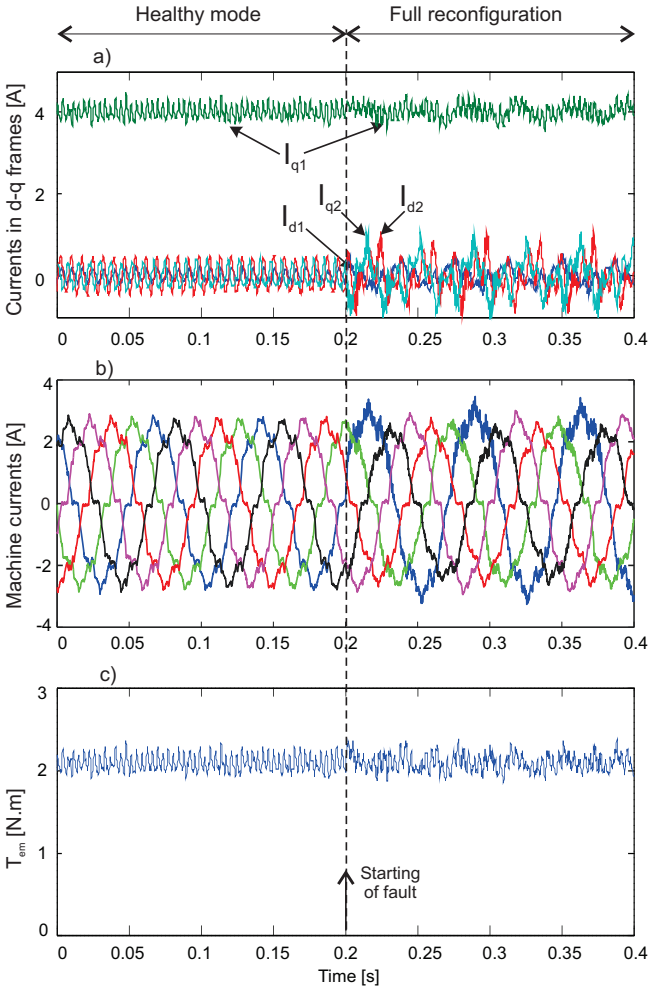

Fig. 16. Inverter switch short-circuit fault after a full reconfiguratio (experimental results). a) Currents expressed in the rotor reference frame; b) Machine currents; c) Electromagnetic torque (calculated from the model).

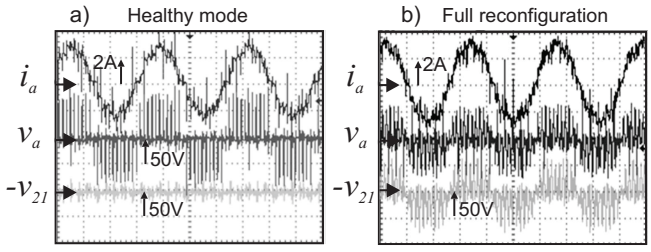

Fig. 17. Healthy operation (a) and full configuratio (b). Scope results showing the faulty a-phase current i_a, the a-phase voltage v_a and the voltage between the two inverter DC-bus v_{21}.

reconfiguratio of switches is not enough to obtain a good result in torque control. It can be noticed that the torque ripple is reduced comparing to Fig. 12 but this value of torque pulsations remains important.

3) Full reconfigu ation: Fig. 16 and Fig. 17 show the experimental results of the control with an inverter switch short-circuit fault after a full reconfiguratio ($\Omega = 42$ rad/s). The fault occurs at time $t = 0.2$ s. In this case, the amplitude of the torque ripple remains the same as in the healthy operation.

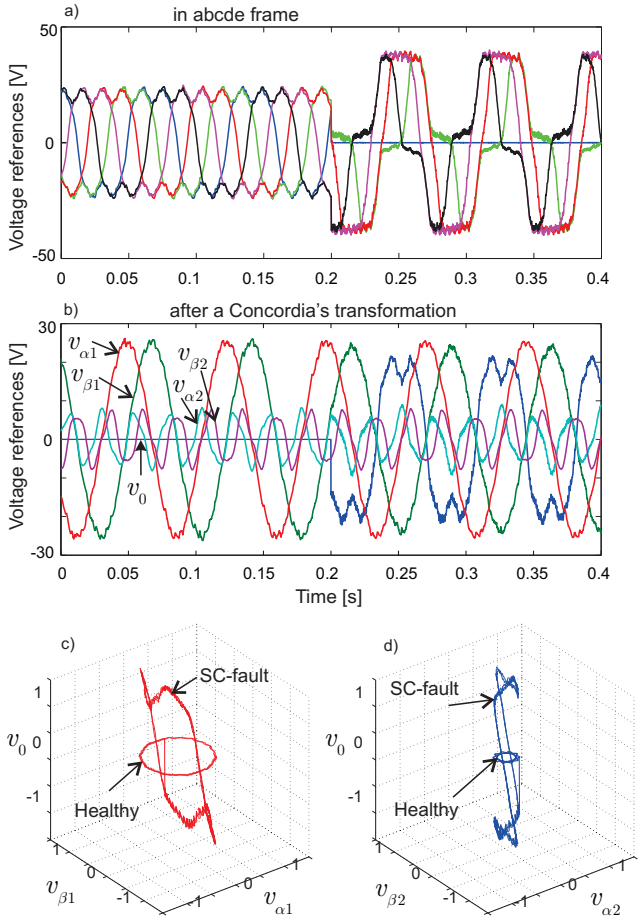

Fig. 18. Inverter switch short-circuit fault (at $t = 0.2$ s) after a full reconfiguratio (experimental results): a) Voltage references of machine in abcde frame; b) References of voltage after a Concordia's transformation; c) Representation of voltages in $\alpha_1\beta_1 v_0$ frame; c) Representation of voltages in $\alpha_2\beta_2 v_0$ frame.

The faulty phase current is quasi-sinusoidal and the machine currents are lightly unbalanced and distorted (see Fig. 16 b)) by comparing to the simulation results (see Fig. 8 b)). In simulation, the bandwidth of the current controller is high enough to compensate the 3^{rd}, the 5^{th} and the 7^{th} harmonics of the back-EMF. In experimentation, these harmonics are not completely compensated (the bandwidth is limited). Therefore, the machine currents are lightly distorted. Furthermore, there is as well the high frequency noise due to the PWM. (22) is verifie as $v_a = -v_{21}$. By imposing this constraint, the new voltage references (for 4 healthy phases) are redetermined. In this case, the voltage of phase-b is a line-line voltage $v_b - v_a = v_{ba}$. Likewise, the voltages of three other phases (c, d and e) are: v_{ca}, v_{da}, v_{ea}. It means that after the fault, the inverter is controlled to obtain the line-line voltages for compensating the phase-a which is faulty. Finally, the machine phase currents are not distorted and maintained as before the fault. These results are shown in Fig. 17.

Fig. 18 gives the machine voltage references and the components of their Concordia transformation. In the healthy operation, a balanced voltage system is obtained as shown in Fig. 18 a). Fig. 18 b) shows that there is no zero sequence

of voltage $v_0 = 0$ in the healthy mode. Therefore, we obtain two circles on two plans $\alpha_1\beta_1$ and $\alpha_2\beta_2$ (Fig. 18 c) and d)). After $t = 0.2$ s, the control strategy takes advantage of the degree of freedom by imposing a zero component of voltage that has no impact on the phase currents and allows the motor to function with the same required torque.

VI. Conclusion

This paper has analyzed the behavior of an open-end five-phase PMSM drive under inverter fault conditions. With a dual-inverter supply, the equivalent five-phase topology offers the possibility to operate the machine under inverter switch short-circuit faults without any additional component. An inherent fault tolerance has been shown in the study. It has also been proved that a simple modificatio of the control algorithm allows the drive to be operated with a constant torque performance operation. Because of the zero voltage component being required, it is obvious that the voltage magnitude that is necessary to maintain a constant torque as before the fault is higher. It is clear that if the voltage constraint is important (maximum voltage), the PMSM speed has to be reduced after the fault. For this purpose, an additional algorithm is necessary to determine a new torque reference while keeping the machine voltage constraints. This work has not been presented here but will be an interesting perspective for future works.

References

[1] S. Yang, D. Xiang, A. Bryant, P. Mawby, L. Ran, and P. Tavner, "Condition monitoring for device reliability in power electronic converters: A review," *IEEE Trans. Pow. Electron.*, vol. 25, no. 11, pp. 2734–2752, 2010.

[2] B. A. Welchko, T. A. Lipo, T. M. Jahns, and S. E. Schulz, "Fault tolerant three-phase ac motor drive topologies: a comparison of features, cost, and limitations," *IEEE Trans. Pow. Electron.*, vol. 19, no. 4, pp. 1108–1116, 2004.

[3] R. R. Errabelli and P. Mutschler, "Fault-tolerant voltage source inverter for permanent magnet drives," *IEEE Trans. Pow. Electron.*, vol. 27, no. 2, pp. 500–508, 2012.

[4] M. Naidu, S. Gopalakrishnan, and T. W. Nehl, "Fault-tolerant permanent magnet motor drive topologies for automotive x-by-wire systems," *IEEE Trans. Ind. Appli.*, vol. 46, no. 2, pp. 841–848, 2010.

[5] F. Richardeau, D. Zhifeng, J. M. Blaquiere, E. Sarraute, D. Flumian, and F. Mosser, "Complete short-circuit failure mode properties and comparison based on igbt standard packaging. application to new fault-tolerant inverter and interleaved chopper with reduced parts count," in *Proceedings of the 14th European Conference on Power Electronics and Applications (EPE 2011)*, 2011, pp. 1–9.

[6] Y. Wang, T. A. Lipo, and D. Pan, "Robust operation of double-output ac machine drive," in *The IEEE 8th International Conference on Power Electronics and ECCE Asia (ICPE & ECCE)*, 2011, pp. 140–144.

[7] B. Mirafzal, "Survey of fault-tolerance techniques for three-phase voltage source inverters," *IEEE Trans. Ind. Electron.*, vol. 61, no. 10, pp. 5192–5202, 2014.

[8] M. Ruba and D. Fodorean, "Analysis of fault-tolerant multiphase power converter for a nine-phase permanent magnet synchronous machine," *IEEE Trans. Ind. Appli.*, vol. 48, no. 6, pp. 2092–2101, 2012.

[9] M. Shahbazi, P. Poure, S. Saadate, and M. R. Zolghadri, "Fault-tolerant five-leg converter topology with fpga-based reconfigurabl control," *IEEE Trans. Ind. Electron.*, vol. 60, no. 6, pp. 2284–2294, 2013.

[10] B. C. Mecrow, A. G. Jack, J. A. Haylock, and J. Coles, "Fault-tolerant permanent magnet machine drives," *Electric Power Applications, IEE Proceedings* -, vol. 143, no. 6, pp. 437–442, 1996.

[11] A. M. El-Refaie, "Fault-tolerant permanent magnet machines: a review," *Electric Power Applications, IET*, vol. 5, no. 1, pp. 59–74, 2011.

[12] J. Zhu and X. Niu, "Investigation of short-circuit fault in a fault-tolerant brushless permanent magnet ac motor drive with redundancy," in *The 5th IEEE Conference on Industrial Electronics and Applications (ICIEA)*, 2010, pp. 1238–1242.

[13] S. Lu and K. Corzine, "Multilevel multi-phase propulsion drives," in *IEEE Electric Ship Technologies Symposium*, 2005, pp. 363–370.

[14] E. Levi, "Multiphase electric machines for variable-speed applications," *IEEE Trans. Ind. Electron.*, vol. 55, no. 5, pp. 1893–1909, 2008.

[15] F. Jen-Ren and T. A. Lipo, "Disturbance-free operation of a multiphase current-regulated motor drive with an opened phase," *IEEE Trans. Ind. Appli.*, vol. 30, no. 5, pp. 1267–1274, 1994.

[16] H. A. Toliyat, "Analysis and simulation of five-phase variable-speed induction motor drives under asymmetrical connections," *IEEE Trans. Pow. Electron.*, vol. 13, no. 4, pp. 748–756, 1998.

[17] F. Meinguet, P. Sandulescu, X. Kestelyn, and E. Semail, "A method for fault detection and isolation based on the processing of multiple diagnostic indices: Application to inverter faults in ac drives," *IEEE Trans. on Vehicular Technology*, vol. 62, no. 3, pp. 995–1009, 2013.

[18] F. Meinguet, E. Semail, and J. Gyselinck, "An on-line method for stator fault detection in multi-phase pmsm drives," in *Vehicle Power and Propulsion Conference (VPPC)*, 2010, pp. 1–6.

[19] X. Kestelyn and E. Semail, "A vectorial approach for generation of optimal current references for multiphase permanent-magnet synchronous machines in real time," *IEEE Trans. Ind. Electron.*, vol. 58, no. 11, pp. 5057–5065, 2011.

[20] F. Locment, E. Semail, and X. Kestelyn, "Vectorial approach-based control of a seven-phase axial flu machine designed for fault operation," *IEEE Trans. Ind. Electron.*, vol. 55, no. 10, pp. 3682–3691, 2008.

[21] D. Flieller, N. K. Nguyen, P. Wira, G. Sturtzer, D. O. Abdeslam, and J. Merckle, "A self-learning solution for torque ripple reduction for nonsinusoidal permanent-magnet motor drives based on artificia neural networks," *IEEE Trans. Ind. Electron.*, vol. 61, no. 2, pp. 655–666, 2014.

[22] D. Flieller, N. K. Nguyen, H. SCHWAB, and G. Sturtzer, "Control of non-conventional synchronous motors. chapter 3: Synchronous machines in degraded mode." ISTE Ltd and John Wiley & Sons Inc., 2012.

[23] S. Dwari and L. Parsa, "Fault-tolerant control of five-phase permanent-magnet motors with trapezoidal back emf," *IEEE Trans. Ind. Electron.*, vol. 58, no. 2, pp. 476–485, 2011.

[24] A. Tani, M. Mengoni, L. Zarri, G. Serra, and D. Casadei, "Control of multiphase induction motors with an odd number of phases under open-circuit phase faults," *IEEE Trans. Pow. Electron.*, vol. 27, no. 2, pp. 565–577, 2012.

[25] N. Bianchi, S. Bolognani, and M. D. Pre, "Design and tests of a fault-tolerant five-phase permanent magnet motor," in *The 37th IEEE Power Electronics Specialists Conference (PESC '06)*, 2006, pp. 1–8.

[26] F. Baudart, B. Dehez, E. Matagne, D. Telteu-Nedelcu, P. Alexandre, and F. Labrique, "Torque control strategy of polyphase permanent-magnet synchronous machines with minimal controller reconfiguratio under open-circuit fault of one phase," *IEEE Trans. Ind. Electron.*, vol. 59, no. 6, pp. 2632–2644, 2012.

[27] F.-J. Lin, Y.-C. Hung, and M.-T. Tsai, "Fault-tolerant control for six-phase pmsm drive system via intelligent complementary sliding-mode control using tskfnn-amf," *IEEE Trans. Ind. Electron.*, vol. 60, no. 12, pp. 5747–5762, Dec 2013.

[28] H. Guzman, M. J. Duran, F. Barrero, B. Bogado, and S. Toral, "Speed control of five-phase induction motors with integrated open-phase fault operation using model-based predictive current control techniques," *IEEE Trans. Ind. Electron.*, vol. 61, no. 9, pp. 4474–4484, 2014.

[29] C. Hang Seng, M. J. Duran, E. Levi, M. Jones, H. Wooi-Ping, and N. Abd Rahim, "Postfault operation of an asymmetrical six-phase induction machine with single and two isolated neutral points," *IEEE Trans. Pow. Electron.*, vol. 29, no. 10, pp. 5406–5416, 2014.

[30] B. A. Welchko, T. M. Jahns, W. L. Soong, and J. M. Nagashima, "Ipm synchronous machine drive response to symmetrical and asymmetrical short circuit faults," *IEEE Trans. Ener. Conver.*, vol. 18, no. 2, pp. 291–298, 2003.

[31] E. Levi, I. N. W. Satiawan, N. Bodo, and M. Jones, "A space-vector modulation scheme for multilevel open-end winding five-phase drives," *IEEE Trans. Ener. Conver.*, vol. 27, no. 1, pp. 1–10, 2012.

[32] C. Lihua, F. Z. Peng, and C. Dong, "A smart gate drive with self-diagnosis for power mosfets and igbts," in *Twenty-Third Annual IEEE Applied Power Electronics Conference and Exposition (APEC 2008)*, 2008, pp. 1602–1607.

[33] W. Arendt, N. Ulrich, T. Werner, and R. Tobias, "Application manual power semiconductors," in *SEMIKRON International GmbH*, 2011.

[34] E. Semail, A. Bouscayrol, and J. P. Hautier, "Vectorial formalism for analysis and design of polyphase synchronous machines," *European Physical Journal-Applied Physics*, vol. 22, no. 3, pp. 207–220, 2003.
[35] L. Parsa and H. A. Toliyat, "Five-phase permanent-magnet motor drives," *IEEE Trans. Ind. Appli.*, vol. 41, no. 1, pp. 30–37, 2005.

Ngac Ky Nguyen received the B.Sc. degree in electrical engineering from Ho Chi Minh City University of Technology, Ho Chi Minh City, Vietnam, in 2005, the M.Sc. degree in electrical and electronic engineering from École Polytechnique de l'Université de Nantes (PolyTech Nantes), Nantes, France, in 2007, and the Ph.D. degree in electrical and electronic engineering from the University of Haute Alsace, Mulhouse, France, in 2010.

From 2011 to 2012, he was with the Department of Electrical Engineering, Institut National des Sciences Appliquées (INSA) of Strasbourg, Strasbourg, France. Since September 2012, he has been an Associate Professor with the Laboratory of Electrical Engineering and Power Electronics of Lille (L2EP), Arts et Métiers ParisTech, Lille, France. His research interests are modeling and control of synchronous motors, power converters and fault-tolerant multiphase machine drives.

Fabien Meinguet received the Master's degree in electrical engineering and the Ph.D. degree from the Université libre de Bruxelles, Brussels, Belgium, in 2007 and 2012, respectively.

From February 2012 to May 2013, he was a Postdoc and Teaching Assistant with the Laboratory of Electrical Engineering and Power Electronics of Lille (L2EP), Arts et Métiers ParisTech, Lille, France. He is currently a Research Engineer with Thales Alenia Space - Thales Group, Belgium. His main research interests are power electronics and fault-tolerant drives, including design, control, and diagnosis.

Eric Semail (M'02) received the M.S. degree from Ecole Normale Supérieure, Paris, France, in 1986 and the Ph.D. degree, with specializations in tools and studying method of polyphase electrical systems and generalization of the space vector theory, from Lille University, Lille, France, in 2000. He is currently with the Laboratory of Electrical Engineering and Power Electronics of Lille (L2EP), Arts et Métiers ParisTech, Lille, where he became an Associate Professor in 2001 and a full Professor in 2010. In L2EP, his field of interest include the design, modeling, and control of multiphase drives (converters and ac drives). More generally, he studies multimachine and multiconverter systems. His application field are automotive, marine, and offshore wind power.

Xavier Kestelyn was born in Dunkerque, France, in 1971. He received the Ph.D. degree in electrical engineering from Lille University, Lille, France, in 2003.

After ten years as a teacher of electrical engineering in high school, he was an Associate Professor for ten years and is currently a Full Professor of electrical engineering with the Laboratory of Electrical Engineering and Power Electronics of Lille (L2EP), Arts et Métiers ParisTech, Lille, France. His research interests include the modeling and control of multiphase drives and new power grid topologies.